JOURNAL OF NEUROTRAUMA
Volume 23, Number 5, 2006

Pp. 721–732

Mass-Related Traumatic Tissue Displacement and Behavior: A Screen for Treatments that Reduces Harm to Bystander Cells and Recovery of Function

HONGYAN YANG,[1,2,4] MARNIE PRESTON,[2] MICHAEL CHOPP,[4,5] FENG JIANG,[4] XUEPENG ZHANG,[4] and TIMOTHY SCHALLERT[1,2,3,4]

ABSTRACT

In this study, we focused on a preclinical model of brain compression injury that has relevance to pathological conditions such as tumor, hematoma, blood clot, and intracerebral bony fragment. We investigated behavioral impairment as a result of rapid-onset small mass, and the factors involved in lesion formation and neuroplasticity. An epidural bead implantation method was adopted. Two sizes (1.5 mm and 2.0 mm thick) of hemisphere-shaped beads were used. The beads were implanted into various locations over the sensorimotor cortex (SMC—anterior, middle and posterior). The effects of early versus delayed bead removal were examined to model clinical neurosurgical or other treatment procedures. Forelimb and hind-limb behavioral deficits and recovery were observed, and histological changes were quantified to determine brain reaction to focal compression. Our results showed that the behavioral deficits of compression were influenced by the location, timing of compression release, and magnitude of compression. Even persistent compression by the thicker bead (2.0 mm) caused only minor behavioral deficits, followed by fast recovery within a week in most animals, suggesting a mild lesion pattern for this model. Brain tissue was compressed into a deformed shape under pressure with slight tissue damage, evidenced by pathological evaluation on hematoxylin and eosin (H&E)– and TUNEL–stained sections. Detectable but not severe behavioral dysfunction exhibited by this model makes it particularly suitable for direct assessment of adverse effects of interventions on neuroplasticity after brain compression injury. This model may permit development of treatment strategies to alleviate brain mass effects, without disrupting neuroplasticity.

Key words: behavior; brain tumor; hematoma; injury; neuroplasticity; recovery of function

INTRODUCTION

BRAIN COMPRESSION—associated with brain injury, tumors, focal edema-induced herniation, and intracranial hemorrhage—is produced by the effect of an additional space-occupying mass within the closed cavity of the skull on the normal brain (mass effect), or mechanical forces during trauma. A mass can block the circulation system for the cerebrospinal fluid, resulting in surrounding brain edema and an even larger mass is formed,

[1]Institute for Neuroscience and [2]Department of Psychology, University of Texas at Austin, Austin, Texas.
[3]Department of Neurosurgery, University of Michigan, Ann Arbor, Michigan.
[4]Department of Neurology, Henry Ford Health Sciences Center, Detroit, Michigan.
[5]Department of Physics, Oakland University, Rochester, Michigan.

which causes compression or displacement of brain tissue. General symptoms associated with mass effect, such as headache and vomiting, are due to increased intracranial pressure, while focal symptoms, involving behavioral and cognitive dysfunctions, such as hemiparesis, aphasias, impulsivity and memory or attentional deficits, depend in part upon which functional areas of the brain are affected.

Chen et al. first developed a novel focal compression model with epidural implantation of a plastic bead over the sensorimotor cortex (SMC), and investigated the morphological changes of the surrounding brain tissue (Chen et al., 2003). Although they reported that no obvious behavioral effects could be detected, it seemed reasonable that if sensitive enough tests were applied, mild deficits might be found in this model, which would enhance its value as a preclinical method to develop single or multi-target interventions that can reduce mass while promoting restorative events that contribute to "quality of life." Here, we focused on the examination of behavioral changes in this focal compression model and the neuroplasticity associated with the mass lesion localized in the SMC, using sensitive tests that can detect injury to this region, recovery of function and small variations in trauma extent. Behavioral deficits depend on which regions of the SMC are injured (Barth et al., 1990b; Baskin et al., 2003). In this study, we observed the location-dependent behavioral effects of the compression injury. Furthermore, we investigated how different magnitudes of compression affect behavioral deficits without causing severe brain tissue damage. In the clinic, surgical resections are often executed to reduce intracerebral pressure in patients suffering from brain trauma, either caused by an injury, brain tumor or hemorrhage. Therefore, we also investigated how different time points for compression release influence functional recovery.

Quality of life after treatment for mass-related insults has not been adequately modeled, particularly functional outcome associated with brain integrity. For example, interventions that target tumor growth, including pro-apoptotic treatments or procedures that interfere with neurogenesis, angiogenesis, mitosis, or trophic factor binding, may potentially exaggerate secondary degeneration or impair neuroplasticity and functional recovery from brain injury associated with the tumor mass or its debulking (Raber et al., 2004). Preclinical studies should better match clinical trials, in which functional outcome is a major target. However, even in the clinic a treatment that is sub-optimal could shrink the mass, improve function and save lives. Without controlling for mass effects specifically, it cannot be determined whether the treatment is maximally benign with respect to surviving brain tissue because the extremely beneficial effects of mass reduction would severely mask any adverse effects of the treatment on brain function (Hua et al., 2005). Moreover, because tumors and other agents that produce mass effects initiate cascades of pathological and non-pathological events that are independent of mass per se, a model that does not initiate these cascades may allow one to investigate behavior-related mass effects independently and thus may be additionally useful.

MATERIALS AND METHODS

Subjects

All animal experimental procedures were approved by the University of Texas at Austin's Institutional Animal Care and Use Committee. A total of 71 male Sprague-Dawley rats (250–350 g) from the University of Texas at Austin's Animal Resources Center were employed in this study. They were housed in pairs in Plexiglas tub cages and were maintained on a 12:12 h light/dark cycle. Prior to the experiment they were tamed by gentle handling, and food and water were available ad libitum.

Materials

Two different sizes of hemispherical plastic beads with different thicknesses (manufactured from an HDPE rod by a local machine shop at the University of Texas, Austin) were used for focal compression surgeries. One is 4.8 mm in diameter and 1.5 mm in thickness, and the other is 4.8 mm in diameter and 2.0 mm in thickness. A small dent was drilled in the center of the flat surface for the convenience of orientation and removal.

Experimental Model

The lesion side was selected opposite to the side of limb that showed bias during baseline testing. Rats were anesthetized with i.p. injections of Ketamine (90 mg/kg) and Xylazine (10 mg/kg). Body temperature was measured and maintained with a heating pad at 37–37.5°C during surgery. The epidural bead implantation surgery was performed as described by Chen et al. (2003). Briefly, each animal was secured to the stereotaxic apparatus (Kopf), the scalp was incised and an elliptical hole with 5.8 mm in long diameter and 3.8 mm in short diameter was drilled in the skull over the SMC. The plastic bead, with the flat surface facing upward, was slipped obliquely into the hole very slowly and carefully to avoid damage to the dura. After the bead was placed completely under the skull, it was pulled back along the short axis of the hole and fixed well into the epidural space. The bead can be inserted and fixed because the diameter of the bead is shorter than the long diameter of the skull

hole but longer than the short diameter of the skull hole. The bead was moved gently using the dent and a needle until the center of the bead was located on the required coordinates. The surgery procedure is shown as Figure 1.

To compare the mechanical compression effects at different locations of the SMC, a plastic bead with 1.5-mm thickness was used, and the rats were divided into three groups. Group 1 (anterior group, $n = 6$) underwent bead implantation with the compression center ~2 mm rostral to the bregma and 2.5 mm lateral to the midline; Group 2 (middle group, $n = 10$) was given bead implantation with the compression center 0.7 mm rostral to the bregma and 2.5 mm lateral to the midline; Group 3 (posterior group, $n = 6$) received bead implantation with the compression center ~2 mm caudal to the bregma and 2.5 mm lateral to the midline.

To detect the compression effects alone and to exclude the influence of the surgical procedure of skull removal on the behavioral results, Group 4 (control group, $n = 9$) was designed to be compared with the group subjected to 1.5-mm-thick bead implantation over the middle SMC. The control group received only skull removal within the same area as the middle group described above, but did not undergo bead implantation.

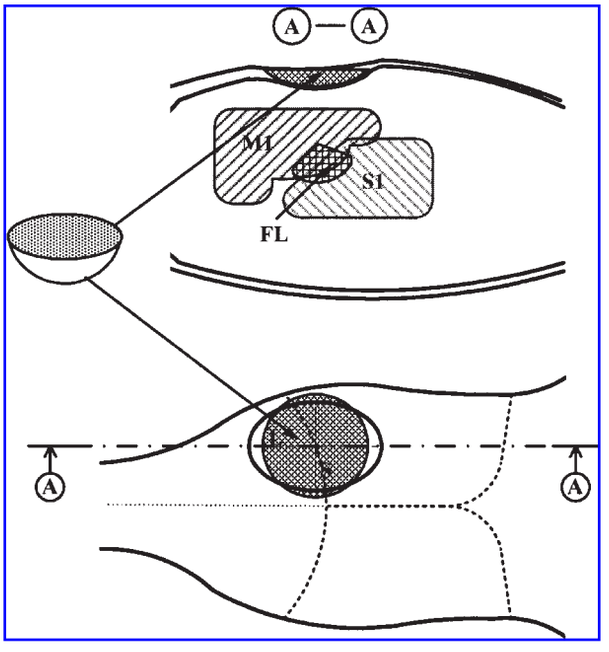

FIG. 1. Schematic diagram demonstrating the epidural bead implantation procedure. Dorsal view and corresponding lateral view of the A-A cross-section are shown. In this diagram, the bead implantation site is approximately the middle sensorimotor cortex (SMC). M1, primary motor cortex; S1, primary sensory cortex; FL, forelimb area of parietal cortex.

To determine the effects of magnitude of compression, plastic beads with 2.0-mm thickness were employed and Group 5 (2.0-mm bead group, $n = 8$) underwent this bead implantation with the same compression center as the 1.5 mm thick bead implantation over the middle SMC.

After the bead implantation or control procedure, the scalp was sutured and the rats were placed in a humidified incubator for recovery.

To examine the effects of compression release at different time points, Group 6 (day 0 removal group, $n = 9$) underwent a 1.5-mm-thick bead implantation over the middle SMC, followed by immediate bead removal, and Group 7 (day 3 removal group, $n = 7$) received a 1.5 mm-thick-bead implantation over the middle SMC, followed by delayed bead removal at post-operative (post-op) day 3. The behavioral results of these two groups were compared with those of the group undergoing persistent 1.5-mm-thick bead compression over the same area.

Behavioral Tests

Forelimb-use asymmetry test (cylinder test). Rats were placed in a transparent cylinder, which is 30 cm high and 20 cm in diameter. Rats tend to rear and contact the wall of the cylinder with their forepaws spontaneously. The number of wall contacts with the ipsilateral (unaffected), the contralateral (affected) and both limbs was recorded by a rater blind to the lesion side. Twenty consecutive behaviors were scored. The extent of forelimb-use asymmetry was calculated as ipsilateral limb use, plus 1/2 the number of "both" contacts, divided by the total number of behaviors (equal to 20). Higher scores (>50%) indicate greater behavioral deficits (Schallert and Woodlee, 2005).

Somatosensory asymmetry test. Rats were tested in their home cage. Adhesive patches (Avery adhesive backed labels, 113 mm^2) were attached to the distal-radial aspect of both forelimbs. Rats tend to remove these uncomfortable stimuli. The order of contact (i.e., left vs. right) was recorded in each of four trials to determine whether the rat showed a bias. If the animal showed a preference for removing the stimulus from one particular forelimb—that is, if the adhesive stimulus was contacted first on 75% or more of the trials—then additional tests were conducted to determine the magnitude of the somatosensory asymmetry. The size of the unbiased limb stimulus was progressively increased and, at the same time, the size of the biased limb stimulus was decreased by an equal amount (14.1 mm^2). The ratio of the size of the unbiased limb stimulus relative to that of the biased limb stimulus was increased until the bias was neutralized, providing the magnitude of somatosensory asymmetry. A score was given to reflect the two levels be-

tween which the animal reversed the original order of contact. Higher scores indicate greater behavioral deficits (Schallert et al., 1982, 2000, 2002; Schallert and Whishaw, 1984).

Foot-fault test. Animals were placed on an elevated grid floor (45 cm × 30 cm), 2.5 cm higher than a solid base floor, with 2.5 cm × 2.5cm diameter openings. When animals inaccurately place a limb, the limb falls through one of the openings in the grid. When the limb fell through and pulled back quickly without touching the solid base, the behavior was called a half fault and counted as one foot-fault score. If the limb fell through and touched the base for support, this situation was called a full fault and counted as two foot-fault scores. Both foot-fault scores and the number of total steps for both forelimbs in a trial with at least 40 movements were measured. The asymmetry score was given by subtracting the percent of ipsilateral forelimb faults from the percent of contralateral forelimb faults (Barth et al., 1990b).

Tapered ledged beam test. A tapered beam, 165 cm long and 2-cm-thick, was placed on top of a wider beam to create a tapered beam with 2-cm-wide ledges on each side positioned 2 cm below the top of the beam surface. This arrangement allows rats traversing the beam to use the bottom ledge as a crutch when they misstep. The ledged beam reduces the need for rapidly learning compensatory motor behaviors to prevent falling, and thus reveals behavioral deficits in the rats chronically (Fleming et al., 2006). If a rat misstepped and its limb touched either side of the beam without using the ledge for support, it was counted as a half fault. If the rat misstepped onto the ledge, it was counted as a full fault. Both step faults and the number of total steps for each hind-limb over five trials across the entire beam were measured. The asymmetry score was calculated by subtracting the percent of ipsilateral hind-limb faults from the percent of contralateral hind-limb faults (Schallert et al., 2002).

Vibrissae-evoked forelimb placing test. A same-side placing response (standard placing test) can be elicited by gently holding the rat by its torso, allowing the forelimbs and hindlimbs to hang free, and brushing the ipsilateral vibrissae against the edge of a table top (Barth et al., 1990a; Jones and Schallert, 1994; Schallert and Woodlee, 2005). To elicit a cross-midline placing response (cross-midline placing test), an experimenter turned the rat sideways and brushed the vibrissae contralateral to the placing forelimb against the surface of the table while gently restraining the other forelimb (Woodlee et al., 2005). Percent successful placing was measured for both forelimbs over 10 trials in both of these two placing tests (Schallert et al., 2000, 2002; Hua et al., 2005).

Tissue Processing and Analysis

Rats were anesthetized with an overdose of pentobarbital (75 mg/kg, i.p.) and perfused through the left ventricle with neutral buffered 10% formalin as a fixative following vascular washout with a 0.1 M heparinized phosphate buffer rinse. Brains were removed and post-fixed at 4°C in the same fixative.

The brain tissue from rats sacrificed at post-op day 7 was processed, embedded, and cut into seven 2-mm-thick coronal blocks. Six-μm-thick paraffin sections from each block containing the area of bead compression were obtained and stained with hematoxylin and eosin (H&E) for evaluation of pathological changes. The paraffin sections were also counter stained with TUNEL Apoptosis Tag kit (Chemicon) and hematoxylin for in situ apoptosis detection according to the manufacturer's instructions. In the TUNEL assay, only cells containing dark brown apoptotic bodies ($>$2) were referred to as apoptotic cells.

The brains from rats sacrificed at post-op day 28 were cut into 50-μm-thick sections on a vibratome. Every fourth section was mounted on slides and stained with toluidine blue for examination of anatomical changes and location. The areas containing the compressive lesion were scanned into the computer. All the variables were measured for both lesioned and corresponding contralateral unlesioned sides. Cortex thickness, hemisphere width, and the volume of both the hemispheres and the cortices were calculated with an NIH image analysis program (ImageJ, NIH). The data are presented as the percentage for each parameter of the lesion side to the corresponding contralateral side.

Statistical Analysis

SPSS (SPSS, Inc.) repeated-measures analysis of variance (ANOVA) was applied to examine behavioral data across days, and the simple main effects at a specific test day were determined with one-way ANOVAs. When there was a significant overall effect, post-hoc analyses were carried out. The anatomical data from different lesion groups were also compared by ANOVA.

RESULTS

SMC Lesion Extent and Placement

Figure 2 shows the brains removed 28 days after the 1.5-mm-thick bead compression over the anterior (Fig. 2A), middle (Fig. 2B), and posterior (Fig. 2C) SMC, respectively. Sampling slices with Nissl staining from the

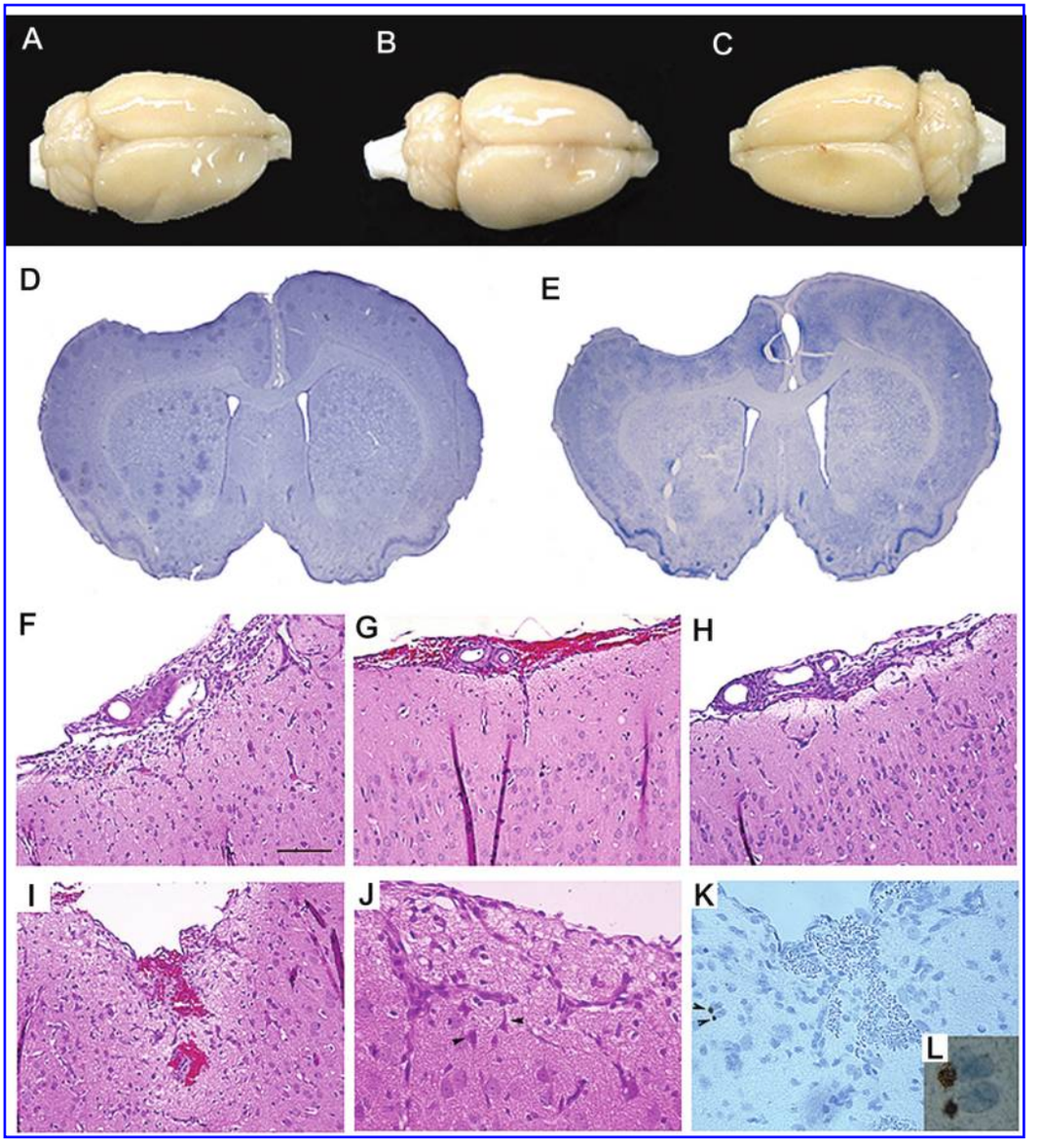

FIG. 2. Histological images. (**A–C**) Brains with 1.5-mm-thick bead compressions over varied areas of the sensorimotor cortex (SMC). These brains were all removed 28 days after bead implantations. (A) Anterior SMC compression. (B) Middle SMC compression. (C) Posterior SMC compression. (**D,E**) Slices at the compression center with Nissl staining. These two slices were both sectioned from brains with bead compressions for 28 days. (D) 1.5-mm-thick bead compression. (E) 2.0-mm-thick bead compression. (**F–L**) Hematoxylin and eosin (H&E) staining and TUNEL apoptosis assay. H&E staining images (×20) show different magnitudes of damage, which includes hemorrhage, edema, and cell death to the brain tissue in representative slices from 1.5-mm-thick bead implantation (F); 1.5-mm-thick bead implantation followed by immediate removal (G); 1.5-mm-thick bead implantation followed by removal at post-op day 3 (H); 2.0-mm-thick bead implantation (I). All were sacrificed at post-op day 7. Panel J shows a higher magnification (×40) of a representative slice from the 2.0-mm-thick bead compression group, with arrow heads indicating samples of necrotic neurons. Hematoxylin and TUNEL counter-staining (×40) shows few apoptosis signals even in the 2.0-mm-thick bead implantation model, sacrificed at post-op day 7 (K). The arrow heads in panel K display samples of apoptotic neurons. Panel L shows a high magnification (×100) of dark brown apoptotic neurons. Scale bar = 100 μm (F–I), 50 μm (J,K), 20 μm (L).

group of 1.5-mm-thick bead compression over the middle SMC (Fig. 2D) and the group of 2.0-mm-thick bead compression over the middle SMC (Fig. 2E) are shown in Figure 2 as well. Both coronal sections were obtained at the site of the approximate compression center of each brain from the corresponding groups sacrificed 28 days after lesions. Anatomical analysis shows that both the 1.5-mm-thick and the 2.0-mm-thick bead compressions led to brain deformation, in which the midline shifted toward the contralateral side and the brain became wider as a result of the compression force. However, little change was found in brain volume. The 2.0-mm-thick bead caused more brain compression compared to the 1.5-mm-thick bead.

Table 1 shows the results for the lesioned hemisphere relative to the unlesioned hemisphere, including cortex thickness at the compression center, mean cortex thickness in the adjacent compression area, hemisphere width at the compression center, mean hemisphere width in the adjacent compression area, and the hemisphere and cortex volumes in the compression area. All data were collected from brains removed 28 days after lesions and subjected to Nissl staining. All three groups of 1.5-mm-thick bead implantations with varied compression locations showed less than 2% cortical tissue loss. One-way ANOVA indicated no significant differences among the anterior, middle and posterior SMC compression groups ($F(2,13) = 0.201$; $p = 0.820$). Compression induced by the 2.0-mm-thick bead over the middle SMC resulted in approximately 7% of cortical tissue loss. Considering cortex thickness, one-way ANOVA showed no significant differences among the three 1.5-mm-thick bead implantation groups in both cortex thickness at the compression center ($F(2,13) = 2.033$; $p = 0.171$) and the mean cortex thickness in the compression area ($F(2,13) = 3.562$; $p = 0.058$). Also, 2.0-mm-thick bead compression over the middle SMC led to a significantly greater decrease of cortex thickness at the compression center, compared with 1.5-mm-thick bead compression over the same location ($F(1,13) = 4.833$; $p < 0.05$). As for the mean hemisphere width in the compression area, no significant differences were found among the three 1.5-mm-thick bead implantation groups ($F(2,13) = 1.960$; $p = 0.180$). Also, no significant differences in mean hemisphere width were revealed between the groups of 2.0-mm-thick and 1.5-mm-thick beads implanted over the middle SMC ($F(1,13) = 0.125$; $p = 0.729$).

To investigate early pathological changes following focal compressions, four rats in each group were sacrificed at post-op day 7. Hematoxylin and eosin staining and TUNEL apoptosis assay were conducted. As shown in H&E stained sections (Fig. 2F–I), hemorrhage, edema and necrosis were present in each lesion group, varied with magnitude, which was related to the extent of compression. Under light microscopy, as shown in Figure 2J, necrotic neurons could be identified as red neurons, exhibiting cytoplastic eosinophilia, or ghost neurons, with complete loss of hematoxylinophilia, due to the features of necrosis, including pyknosis, karyorrhexis and karyolysis (Garcia et al., 1995). Vacuolization was prominent in the tissue area adjacent to the compressive mass. Active proliferation of blood vessels was also found, presumably reflecting damage-induced neuroplasticity. General pathological evaluation indicated that the 2.0-mm-thick bead compression led to greater brain tissue damage than the 1.5-mm-thick bead compression, while the 1.5-mm-thick bead compression released at post-op

Table 1. Histological Analysis[a]

Ratio (lesion/contralateral)	*1.5 mm bean (an)*	*1.5 mm bead (mid)*	*1.5 mm bead (pos)*	*2.0 mm bead (mid)*
Cortex thickness at the compression center	67.79% ± 0.060	55.86% ± 0.023	58.00% ± 0.053	43.74% ± 0.047
Mean cortex thickness	78.60% ± 0.023	72.10% ± 0.009	74.00% ± 0.028	66.09% ± 0.029
Hemisphere width at the compression center	109.84% ± 0.008	103.22% ± 0.025	103.13% ± 0.009	107.32% ± 0.012
Mean hemisphere width	108.29% ± 0.017	104.95% ± 0.021	102.58% ± 0.008	105.77% ± 0.012
Hemisphere volume	99.58% ± 0.002	96.58% ± 0.009	98.84% ± 0.004	93.93% ± 0.019
Cortex volume	99.05% ± 0.009	98.01% ± 0.013	98.61% ± 0.013	93.20% ± 0.024

[a]Ratios of cortex thickness at the compression center, the mean cortex thickness in the compression area, hemisphere width at the compression center, the mean hemisphere width in the compression area, hemisphere volume and cortex volume in the compression area of the lesion side to the contralateral side are shown from different lesion types, including 1.5-mm-thick bead implantation over the anterior (an) sensorimotor cortex (SMC), middle (mid) SMC, and posterior (pos) SMC, and 2.0-mm-thick bead implantation over the middle SMC. All the data were collected 28 days after surgeries with sections Nissl-stained. Data are mean ±SEM.

day 3 displayed reduced brain tissue damage compared with the 1.5-mm-thick bead that remained implanted. The 1.5-mm-thick bead compression released immediately resulted in minor but notable brain tissue damage. With TUNEL staining, only few apoptotic cells were found even in the 2.0-mm-thick bead compression group (Fig. 2K,L), suggesting that little apoptosis is involved in such focal compression lesions.

Behavioral Deficits of Compression Are Dependent on Implant Locations

As shown in Figure 3, focal-compression-induced behavioral deficits were dependent upon insult location. The 1.5-mm-thick beads were implanted into the epidural space over the anterior, middle or posterior SMC. In the cylinder test, for post-op day 4, one-way ANOVA among the four groups revealed a significant main effect ($F(3,27) = 3.862; p < 0.05$). Post-hoc analyses indicated a significant difference between the middle SMC bead implant group and the control group ($F(1,17) = 8.303$; $p < 0.05$). However, no significant differences were found either between the anterior group and the control ($F(1,13) = 0.011$; $p = 0.918$) or between the posterior group and the control ($F(1,13) = 0.478$; $p = 0.502$). Also, at post-op day 4, the middle SMC bead implant group showed significantly more behavioral deficits than the anterior SMC bead implant group ($F(1,14) = 7.064$; $p < 0.05$), but there were no significant differences between either the middle group and the posterior group ($F(1,14) = 4.456$; $p = 0.053$), or the anterior group and the posterior group ($F(1,10) = 0.372$; $p = 0.556$). Because focal compression over the middle SMC led to more consistent behavioral deficits, the following experiments investigated the influence of timing and magnitude on compressive effects using the middle SMC bead implantation procedure.

Behavioral Deficits are Dependent on the Timing of Compression Release

In the cylinder test (Fig. 4A), one-way ANOVA showed that 1.5-mm-thick bead implantation led to significant behavioral deficits, compared with the control group at post-op day 4 ($F(1,17) = 8.303$; $p < 0.05$). Compared with the control group, the group with the 1.5-mm-thick bead removed at post-op day 3 showed significant behavioral deficits at post-op day 2 ($F(1,14) = 7.762$; $p < 0.05$), but no significant differences at post-op day 4 and day 7, reflecting that compression release in the early stage can accelerate the functional recovery. When removed immediately after implantation, the 1.5-mm-thick bead did not induce any behavioral deficits in the cylinder test at each time point compared with the control group.

The somatosensory asymmetry test also revealed a similar behavioral pattern (Fig. 4B). One-way ANOVA showed that 1.5-mm-thick bead implantation caused significant behavioral deficits at post-op day 7, compared with the control group ($F(1,17) = 7.382$; $p < 0.05$). Repeated-measures ANOVA showed significant differences between the group with the 1.5-mm-thick bead removed at post-op day 3 and the group with the 1.5-mm-thick bead left in place ($F(1,15) = 6.810$; $p < 0.05$). Simple main effects revealed significant group differences at post-op day 4 ($F(1,15) = 12.937$; $p < 0.01$), suggesting the compression release effects. In contrast to the cylinder test results, the immediate bead removal group

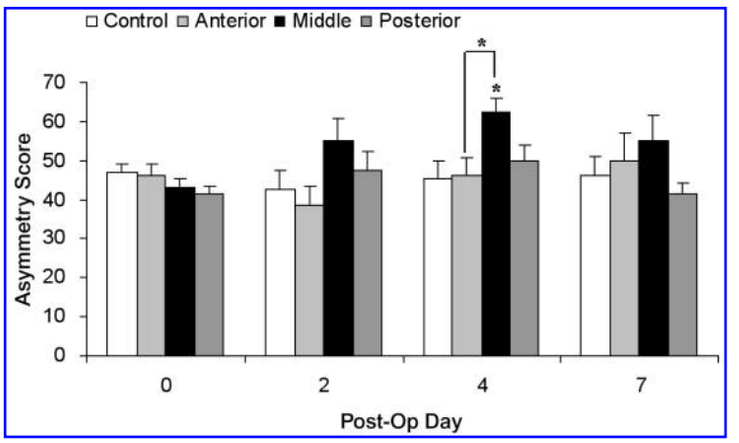

FIG. 3. Forelimb-use asymmetry as measured in the cylinder test. Animals with 1.5-mm-thick bead compression over the middle sensorimotor cortex (SMC), but not those undergoing either anterior or posterior SMC focal compression were found to exhibit significant behavioral asymmetry compared to the control. Data are mean ± SEM. *Significant difference from control or between different conditions with $p < 0.05$.

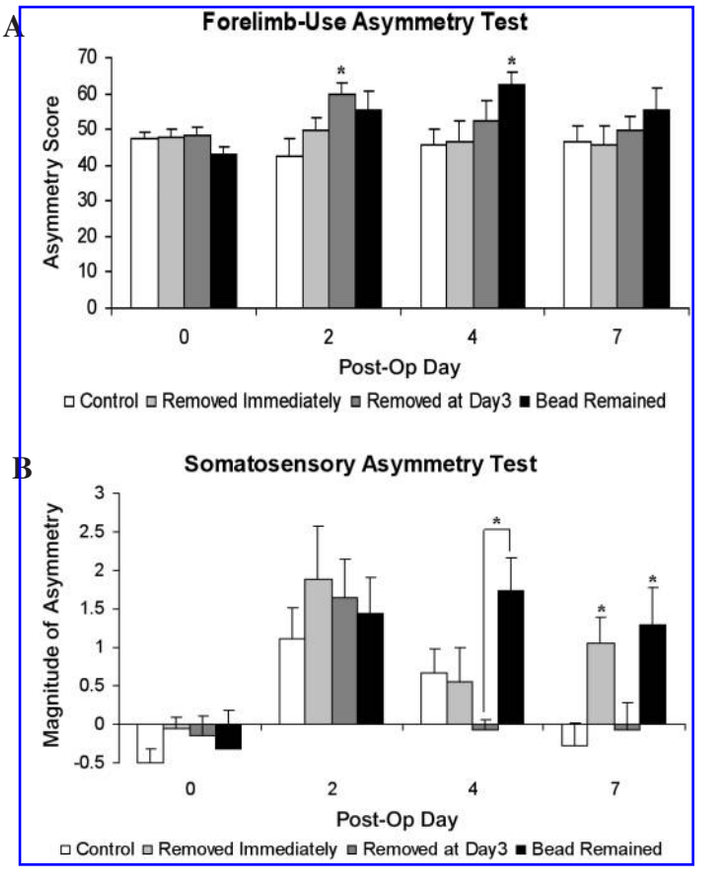

FIG. 4. Forelimb use (**A**) and somatosensory (**B**) asymmetry. 1.5-mm-thick bead implantation caused significant behavioral deficits compared to the control group in both the cylinder test and the somatosensory asymmetry test. Bead removal at post-op day 3 resulted in improved functional recovery in both the cylinder test and the somatosensory asymmetry test. Bead implantation followed by immediate removal caused no behavioral deficits in the cylinder test, but significant deficits in the somatosensory asymmetry test. Data are mean ± SEM. In the somatosensory asymmetry test, a positive number represents a bias ipsilateral to the lesion and a negative number represents a bias contralateral to the lesion. *Significant difference from control or between different conditions with $p < 0.05$.

showed significant somatosensory asymmetry at post-op day 7, compared with the control group ($F(1,16) = 8.965$; $p < 0.01$), suggesting that even transient compression can cause at least some lasting, or delayed, behavioral deficits.

Behavioral Deficits of Compression Depend on the Magnitude of Compression

In order to detect the influence of compression magnitude on behavioral changes, two different sizes of beads were implanted over the middle SMC, and several kinds of behavioral tests were conducted. In the cylinder test, no significant differences were found between the 1.5-mm-thick and 2.0-mm-thick bead implantations. In the somatosensory asymmetry test (Fig. 5A), the 2.0-mm-thick bead caused significantly greater behavioral deficits than the 1.5-mm-thick bead at post-op day 2 ($F(1,16) = 4.739$; $p < 0.05$). In the foot-fault test (Fig. 5B), the 2.0-mm-thick bead implantation also produced significantly greater behavioral deficits than 1.5-mm-thick bead compression at post-op day 2 ($F(1,14) = 6.792$; $p < 0.05$). In the hind-limb ledged tapered beam test (Fig. 5C), repeated-measures ANOVA showed a significant group effect ($F(1,12) = 6.861$; $p < 0.05$). One-way ANOVA revealed that 2.0-mm-thick bead compression resulted in greater behavioral deficits than 1.5-mm-thick bead compression at post-op day 2 ($F(1,12) = 5.626$; $p < 0.05$).

The 1.5-mm-thick bead group did not show any placing deficits. In contrast, the 2.0-mm-thick bead implantation caused significant deficits in contralateral forelimb placing. In the standard placing test (Fig. 5D), repeated-

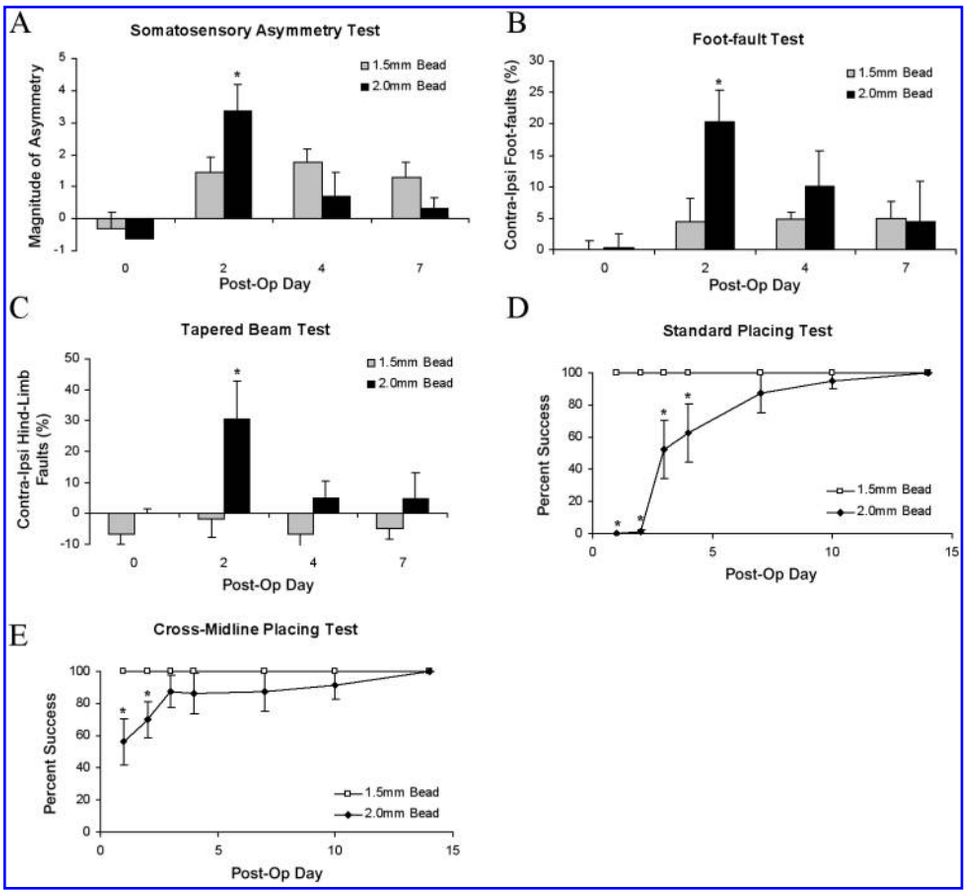

FIG. 5. Somatosensory asymmetry (**A**), foot-faults asymmetry (**B**), hind-limb faults asymmetry as measured in the tapered beam test (**C**), standard placing (**D**), and cross-midline placing (**E**) with the contralateral forelimb following different size bead implantations. The 2.0-mm-thick bead was found to cause greater behavioral deficits than the 1.5-mm-thick bead in all the above tests. Data are mean ± SEM. In A–C, a positive number represents a bias ipsilateral to the lesion and a negative number represents a bias contralateral to the lesison. *Significant difference between different lesion groups with $p < 0.05$.

measures ANOVA showed significant differences between the 1.5-mm-thick bead group and the 2.0-mm-thick bead group ($F(1,16) = 55.591$; $p < 0.001$). There was also a significant time effect ($F(6,96) = 24.581$; $p < 0.001$) and a significant time by group effect ($F(6,96) = 24.581$; $p < 0.001$). Follow-up tests of simple main effects revealed significant group differences at post-op day 1 ($p < 0.001$), day 2 ($p < 0.001$), day 3 ($p < 0.01$), and day 4 ($p < 0.05$). The cross-midline placing test also showed a similar behavioral pattern (Fig. 5E). In repeated-measures ANOVA, there was a significant group effect ($F(1,16) = 5.153$; $p < 0.05$), a significant time effect ($F(6,96) = 5.348$; $p < 0.001$) and a significant time by group effect ($F(6,96) = 5.348$; $p < 0.001$). Follow-up tests of simple main effects revealed significant group differences at post-op day 1 ($p < 0.01$) and day 2 ($p < 0.05$).

DISCUSSION

Besides the bead model that we used in this study, two other models of focal cerebral compression using different devices have been reported in the literature. One is the balloon model, used to examine the intracranial pressure and cerebral blood flow changes in compressed brain tissue (Abe et al., 1984; Douzinas et al., 1999; Im et al., 2002). Another one is the piston model, used to determine the pathological and behavioral effects of acute epidural pressure leading to transient cerebral ischemia (Kundrotienbe et al., 2002, 2004a,b). In 2003, Chen et al. first developed this bead model and used it to investigate how epidural compression affects neuronal morphology. However, no gross behavioral deficits were detected (Chen et al., 2003). The balloon model can be used to mimic mass effect, but is primarily designed for short-

term measurements because the balloon is inflated and deflated acutely. The piston model is designed to mirror transient mechanical disruption of blood vessels during trauma. In the present study, our aim was to investigate the behavioral changes during long-term mass lesions. Chen's bead model can well mimic mass lesions with the bead remaining implanted epidurally for a long time, which allows for the implementation of various interventions and chronic behavioral measurements using sensitive test. Since location, duration and magnitude are the primary factors determining brain mass effects, we further modified the design of the bead by varying its thickness and adding a dent on the flat upper surface for more accurate orientation and more convenient translocation.

The results of the present study suggest that displacement of brain tissue occurs as a result of its elastic property under the insult of focal compression. In general, the brain can adapt to compressive force through deformation (i.e., midline shift and extension within the skull). Our data show that although the thickness of the cortex under compression shrinks significantly, only a small amount of brain tissue loss develops—that is, 2% and 7% of tissue loss a month after 1.5-mm-thick and 2.0-mm-thick bead implantation, respectively. A previous study showed that total dendritic length as well as dendritic spines on all dendrites are reduced, while the densities of neurons and capillaries increased following compression (Chen et al., 2003). Based on the increased densities of neurons and vessels, it was concluded that no cell death was involved in the compression of particles 1.5 mm in thickness (Chen et al., 2003). In our study, H&E staining revealed necrotic cell death and angiogenesis, suggesting ischemia and ischemia-related neuroplasticity. In this case, H&E staining may be a sensitive method of detecting pathological changes.

Previous findings of spine loss accompanied by brain compression suggest that synaptic function may be compromised (Chen et al., 2003). In the present study, our main interest focused on the behavioral changes after focal compression. To detect the influence of location, magnitude and duration of brain compression on behavioral deficits, we changed one factor and fixed the others. We found that a bead implanted over the middle part of the SMC causes reliably detectable behavioral deficits, compared with implantation over either the anterior or the posterior part of the SMC, whereas the shrinkage of the cortical thickness and the loss of cortical volume revealed no significant differences among these three groups. Several previous studies have found that location could be an important variable in behavioral responses in different kinds of lesion models. Varying the location of brain injury in the region of the SMC produced different behavioral outcomes and delayed subcortical degenerative patterns that were influenced by pharmacological interventions (Barth et al., 1990 b; Jones and Schallert, 1992). Baskin et al. (2003), using similar tests, recently showed insult-location-dependent behavioral variation in a mouse traumatic brain injury model. Trauma centered on the middle SMC location appeared to cause the most severe and persistent behavioral deficits (Baskin et al., 2003).

Our data revealed that behavioral deficits depend on the magnitude of brain compression. In our experiment, the 2.0-mm-thick bead caused more brain tissue loss and greater behavioral deficits compared with the 1.5-mm-thick bead after implantation. Note, though, that while both the 1.5-mm-thick and 2.0-mm-thick bead compression induced behavioral deficits in the cylinder test and the somatosensory asymmetry test, only the 2.0-mm-thick bead implantation caused dysfunction in the vibrissae-evoked placing test, which typically can detect only larger injuries. There is extensive evidence, of course, that behavioral deficits depend on the magnitude of subtotal injury. For example, a relationship exists between the extent of dopamine depletion and behavioral deficits in a parkinsonian animal model (Schallert and Tillerson, 2000; Bergstrom et al., 2001), and also, behavioral asymmetries tend to rely on the size of the lesion in a focal cortical ischemia model (Lindner et al., 2003; Allred et al., 2004). Here, we show a relationship between behavioral changes and the extent of brain compression.

Early removal following 1.5-mm-thick bead compression at post-op day 3 showed functional improvement, compared with persistent compression using the same size bead, suggesting that early release of brain compression may be beneficial to functional recovery. After the 1.5-mm-thick bead was removed at post-op day 3, the shape of the brain appeared to recover to its original state by the time of sacrifice. Concurrent with our behavioral findings, Chen's recent study reported that decompression for 14 days resulted in near complete to partial recovery of the cortical thicknesses and the dendritic length of pyramidal neurons, and also, the recoverability was dependent on duration of preceding compression (Chen et al., 2004). It would be important in the future to assess whether motor experience might influence molecular, structural and functional outcome (Jones and Schallert, 1994; Keyvani and Schallert, 2002; Kleim et al., 2003).

After a month's observation, we found that rats with both 1.5-mm-thick and 2.0-mm-thick bead compressions showed only minor behavioral deficits and recovered within 2 weeks, suggesting a mild lesion pattern for this model. We removed the same area of skull as a control operation, which showed transient detectable behavioral asymmetries in the somatosensory asymmetry test, but

the response was normal in the cylinder test. This result is consistent with previous findings that even skull removal can result in behavioral asymmetries (Adams et al., 1994). The effects of transient brain compression were also investigated. Animals with transient 1.5-mm-thick bead implantation followed by immediate removal showed considerable behavioral asymmetries on the somatosensory asymmetry test, but no detectable deficits in the cylinder test, indicating that even transient compression as short as 10 min can lead to detectable behavioral deficits. It may seem paradoxical that significant somatosensory asymmetry was detected in the immediate removal group, compared with the control at post-op day 7, while the day-3 removal group had recovered by day 7. The mechanism to explain this phenomenon remains obscure so far, although secondary damage may possibly play a role in exaggerating brain injury following transient compression through bead-removal induced swelling and ischemia initiated at a critical time point. Chen et al (2004) found that decompression after 3 days or months led to varied extent of recovery of the dendritic length. Perhaps removing the bead early after the implantation can be especially traumatic. Results from earlier investigations showed behavioral deficits up to 7 days on the beam walking test after transient focal compression with a piston for 30 min (Kundrotienbe et al., 2002, 2004a). Taken together, our behavioral data from control operations and transient focal compression indicate that the somatosensory asymmetry test is sensitive even for a slight insult to SMC.

The bead model discussed here may be applied in evaluating treatment effects on neuroplasticity after mass compression in brain tumors, hemorrhage and traumatic head injuries (Yang et al., 2006). Exogenous NGF has been reported to enhance restoration of the density of dendritic spines on pyramidal neurons subjected to compression (Chen et al., 2004). Treatments to remove compressive masses either by pharmaceuticals or by surgery may not promote neuroplasticity or may even damage the self-repair mechanisms involved in mass lesions depending on the timing (Yang et al., 2006). The mild lesion pattern makes this model specifically suitable to detect treatment-induced adverse neurological effects, thereby facilitating an improvement of therapeutic strategies.

CONCLUSION

We modified and further characterized the focal epidural compression model of Chen et al. (Chen et al., 2003) using two different thicknesses of beads, varied implant locations above the SMC and bead removal at different time points. We demonstrated that behavioral deficits depend on the location, magnitude and duration of the focal compression and this focal compression model leads to only a mild injury to the brain. This model may allow investigators to examine directly whether therapies designed to shrink mass would affect brain plasticity and functional recovery independent of mass reduction.

ACKNOWLEDGMENTS

We would like to thank Kartik Rajagopalan and Rebecca Feng for help with behavioral testing; Cynthia Roberts H.T. and Qing-e Lu for assistance with histology; Gabriela Redwine for assistance in editing this manuscript; and Dr. Theresa A. Jones and Dr. Yi Li for their helpful comments regarding the histology evaluation. This study was supported by NIH (grants NS19608, NS23979, NS24707, and NS042345).

REFERENCES

ABE, T., BLACK, P.M., and FOLEY, L. (1984). Changes in parenchymal and ventricular pressure with experimental epidural compression. Surg. Neurol. **22,** 477–480.

ADAMS, F.S., SCHWARTING, R.K., and HUSTON, J.P. (1994). Behavioral and neurochemical asymmetries following unilateral trephination of the rat skull: is this control operation always appropriate? Physiol. Behav. **55,** 947–952.

ALLRED, R.P., and JONES, T.A. (2004). Unilateral ischemic sensorimotor cortical damage in female rats: forelimb behavioral effects and dendritic structural plasticity in the contralateral homotopic cortex. Exp. Neurol. **190,** 433–445.

BARTH, T.M., GRANT, M.L., and SCHALLERT, T. (1990a). Effects of MK-801 on recovery from sensorimotor cortex lesions. Stroke **21,** Suppl 11, III153–III157.

BARTH, T.M., JONES, T.A., and SCHALLERT, T. (1990b). Functional subdivisions of the rat somatic sensorimotor cortex. Behav. Brain Res. **39,** 73–95.

BASKIN, Y.K., DIETRICH, W.D., and GREEN, E.J. (2003). Two effective behavioral tasks for evaluating sensorimotor dysfunction following traumatic brain injury in mice. J. Neurosci. Methods. **129,** 87–93.

BERGSTROM, B.P., SCHERTZ, K.E., WEIRICK, T., et al. (2001). Partial, graded losses of dopamine terminals in the rat caudate-putamen: an animal model for the study of compensatory adaptation in preclinical parkinsonism. J. Neurosci. Methods **106,** 15–28.

CHEN, J.R., WANG, Y.J., and TSENG, G.F. (2003). The effect of epidural compression on cerebral cortex: a rat model. J. Neurotrauma **20,** 767–780.

CHEN, J.R., WANG, Y.J., and TSENG, G.F. (2004). The effects of decompression and exogenous NGF on compressed cerebral cortex. J. Neurotrauma **21,** 1640–1651.

DOUZINAS, E.E., KOSTOPOULOS, V., KYPRIADES, E., et al. (1999). Brain eigenfrequency shifting as a sensitive index of cerebral compliance in an experimental model of epidural hematoma in the rabbit: preliminary study. Crit. Care Med. **27,** 978–984.

FLEMING, S.M., GREEN, E., and SCHALLERT, T. (2006). A ledged-beam walking test for chronic limb deficits after MCAo or other unilateral cortical or striatal injury. Behav. Brain Res. (in press).

GARCIA, J.H., LIU, K.F., and HO, K.L. (1995). Neuronal necrosis after middle cerebral artery occlusion in Wistar rats progresses at different time intervals in the caudoputamen and the cortex. Stroke **26,** 636–642.

HUA, Y., TANG, L., KEEP, R.F., et al. (2005). The role of thrombin in gliomas. J. Thromb. Haemost. **3,** 1917–1923.

HUA, Y., WU, J., PECINA, S., et al. (2005). Ischemic preconditioning procedure induces behavioral deficits in the absence of brain injury? Neurol. Res. **27,** 261–267.

IM, J.J., and PARK, B.R. (2002). Does oxygen deficit to the cerebral blood flow caused by subdural hematoma and/or increased intracranial pressure affect the variations in auditory evoked potentials in white New Zealand rabbits? Neurosci. Lett. **14,** 139–142.

JONES, T.A., and SCHALLERT, T. (1992). Subcortical deterioration after cortical damage: effects of diazepam and relation to recovery of function. Behav. Brain Res. **51,** 1–13.

JONES, T.A., and SCHALLERT, T. (1994). Use-dependent growth of pyramidal neurons after neocortical damage. J. Neurosci. **14,** 2140–2152.

KEYVANI, K., and SCHALLERT, T. (2002). Plasticity-associated molecular and structural events in the injured brain. J. Neuropathol. Exp. Neurol. **61,** 831–840.

KLEIM, J.A., JONES, T.A., and SCHALLERT, T. (2003). Motor enrichment and the induction of plasticity before or after brain injury. Neurochem. Res. **28,** 1757–1769.

KUNDROTIENE, J., CEBERS, G., WAGNER, A., and LILJEQUIST, S. (2004a). The NMDA NR2B subunit-selective receptor antagonist, CP-101, 606, enhances the functional recovery and reduces brain damage after cortical compression-induced brain ischemia. J. Neurotrauma **21,** 83–93.

KUNDROTIENE, J., WAGNER, A., and LILJEQUIST, S. (2002). Extradural compression of sensorimotor cortex: a useful model for studies on ischemic brain damage and neuroprotection. J. Neurotrauma **19,** 69–84.

KUNDROTIENE, J., WAGNER, A., and LILJEQUIST, S. (2004b). Fluoro-Jade and TUNEL staining as useful tools to identify ischemic brain damage following moderate extradural compression of sensorimotor cortex. Acta Neurobiol. Exp. **64,** 153–162.

LINDNER, M.D., GRIBKOFF, V.K., DONLAN, N.A., and JONES, T.A. (2003). Long-lasting functional disabilities in middle-aged rats with small cerebral infarcts. J. Neurosci. **23,** 10913–10922.

RABER, J., FAN, Y., MATSUMORI, Y., et al. (2004). Irradiation attenuates neurogenesis and exacerbates ischemia-induced deficits. Ann. Neurol. **55,** 381–389.

SCHALLERT, T., and TILLERSON, J.L. (2000). Intervention strategies for degeneration of dopamine neurons in parkinsonism: optimizing behavioral assessment of outcome, in: *Central Nervous System Diseases: Innovative Animal Models from Lab to Clinic.* D.F. Emerich, R.L. Dean III, and P.R. Sanberg (eds), Humana Press: Totowa, NJ, pps. 131–151.

SCHALLERT, T., and WHISHAW, I.Q. (1984). Bilateral cutaneous stimulation of the somatosensory system in hemidecorticate rats. Behav. Neurosci. **98,** 518–540.

SCHALLERT, T., and WOODLEE, M.T. (2005). Motor systems: orienting and placing, in: *The Behavior of the Laboratory Rat: A Hand Book with Tests.* I.Q. Whishaw, and B. Kolb (eds), Oxford University Press: New York, pps. 129–140.

SCHALLERT, T., FLEMING, S.M, LEASURE, J.L., TILLERSON, J.L., and BLAND, S.T. (2000). CNS plasticity and assessment of forelimb sensorimotor outcome in unilateral rat models of stroke, cortical ablation, parkinsonism and spinal cord injury. Neuropharmacology **39,** 777–787.

SCHALLERT, T., UPCHURCH, M., LOBAUGH, N., et al. (1982). Tactile extinction: distinguishing between sensorimotor and motor asymmetries in rats with unilateral nigrostriatal damage. Pharmacol. Biochem. Behav. **16,** 455–462.

SCHALLERT, T., WOODLEE, M.T., and FLEMING, S.M. (2002). Disentangling multiple types of recovery from brain injury, in: *Pharmacology of Cerebral Ischemia 2002.* J. Krieglstein and S. Klumpp (eds), Medpharm Scientific Publishers: Stuttgart, pps. 201–216.

WOODLEE, M.T., ASSEO-GARCIA, A.M., ZHAO, X., LIU, S.J., JONES, T.A., and SCHALLERT, T. (2005). Testing forelimb placing "across the midline" reveals distinct, lesion-dependent patterns of recovery in rats. Exp. Neurol. **191,** 310–317.

YANG, H., CHOPP, M., JIANG, F., et al. (2006). Interruption of functional recovery by the NMDA glutamate antagonist MK801 after compression of the sensorimotor cortex: implications for treatment of tumors or other mass-related brain injuries. Exp. Neurol. (in press).

YANG, H., ZHANG, X., CHOPP, M., JIANG, F., and SCHALLERT, T. (2006). Local fluorouracil chemotherapy interferes with neural and behavioral recovery after brain tumor-like mass compression. Behav. Brain Res. (in press).

Address reprint requests to:
Timothy Schallert, Ph.D.
Department of Psychology
University of Texas at Austin
1 University Station, #A8000
Austin, TX 78712

E-mail: tschallert@mail.utexas.edu